Semiconductor Physics, Quantum Electronics & Optoelectronics, 2023. V. 26, No 1. P. 005-016.

Semiconductor physics

Modeling of characteristics of highly efficient textured solar cells based on c-silicon. The influence of recombination in the space charge region

A.V. Sachenko[1], V.P. Kostylyov[1], V.M. Vlasiuk[1], I.O. Sokolovskyi[1], M.A. Evstigneev[2], T.V. Slusar[3], V.V. Chernenko[1]

[1]*V. Lashkaryov Institute of Semiconductor Physics, NAS of Ukraine, 41, prospect Nauky, 03680 Kyiv, Ukraine*
[2]*Department of Physics and Physical Oceanography, Memorial University of Newfoundland, St. John's, NL, A1B 3X7, Canada*
[3]*Electronics and Telecommunications Research Institute, 218, Gajeong-ro, Yuseong-gu, Daejeon 34129, South Korea*
Corresponding author e-mail: viktorvlasiuk@gmail.com

Abstract. Theoretical modeling of the optical and photovoltaic characteristics of highly efficient textured silicon solar cells (SC), including short-circuit current, open-circuit voltage and photoconversion efficiency, has been performed in this work. In the modeling, such recombination mechanisms as non-radiative exciton recombination relative to the Auger mechanism with the participation of a deep recombination level and recombination in the space charge region (SCR) was additionally taken into account. In a simple approximation, the external quantum efficiency of the photocurrent for the indicated SC in the long-wavelength absorption region has been simulated. A theory has been proposed for calculating the thickness dependences of short-circuit current, open-circuit voltage and photoconversion efficiency in them. The calculated dependences are carefully compared with the experimental results obtained for SC with the p^+-i-α-Si:H/n-c-Si/i-n^+-α-Si:H architecture and the photoconversion efficiency of about 23%. As a result of this comparison, good agreement between the theoretical and calculated dependences has been obtained. It has been ascertained that without taking into account recombination in SCR, a quantitative agreement between the experimental and theoretical light *I-V* characteristics and the dependence of the output power in the SC load on the voltage on it cannot be obtained. The proposed approach and the obtained results can be used to optimize the characteristics of textured SC based on monocrystalline silicon.

Keywords: silicon solar cell, theoretical modeling, external quantum efficiency of the photocurrent, short-circuit current, open-circuit voltage, photoconversion efficiency.

https://doi.org/10.15407/spqeo26.01.005
PACS 88.40.hj, 88.40.jj

Manuscript received 30.12.22; revised version received 05.02.23; accepted for publication 08.03.23; published online 24.03.23.

1. Introduction

In the work [1], an experimental study of the thickness dependence of the external quantum efficiency and key parameters of highly efficient textured heterojunction solar cells (SC) with the p^+-i-α-Si:H/n-c-Si/i-n^+-α-Si:H architecture, such as short-circuit current density, open-circuit voltage, filling factor and photoconversion efficiency, has been performed. The resulting dependences were qualitatively explained using the ray tracing approach [2]. In our work [3], an approach was proposed, which, in principle, allows us to quantitatively agree the experimental dependences obtained in the work [1] with the theory. For this, first, it is necessary to use the empirical dependence for the external quantum efficiency in the long-wave absorption region proposed in the work [4].

Second, when considering the recombination mechanisms in silicon, in addition to those that are usually considered, it is necessary to take into account the mechanism of non-radiative exciton recombination through a deep impurity center [5] and the mechanism of recombination in SCR [6, 7]. If the mechanism of non-radiative exciton recombination through a deep impurity center [5] makes a contribution to the effective lifetime of SC studied in [1], which is comparable to the contribution of radiative recombination, then the recombination mechanism in SCR is much more significant. As shown in the work, without taking it into account, a quantitative agreement between experimental and theoretical light *I–V* characteristics and load characteristics for SC studied in [1] cannot be obtained.

The theory developed in [3] in a one-dimensional approximation makes it possible to obtain the values of photoconversion efficiency η and other key parameters of textured silicon SC, such as, in particular, short-circuit current I_{SC}, open-circuit voltage V_{OC}, and *I–V* filling factor *FF*. It is valid when the following criteria are met: 1) $L_d >> d$, 2) $S_S << D_A/d$, where L_d is the diffusion length of electron-hole pairs, *d* – thickness of the SC base, S_S – total rate of surface recombination on the front and back surfaces, D_A – ambipolar diffusion coefficient. When implementing these criteria, you can ignore the spatial dependence of the concentration of excess non-equilibrium charge carriers $\Delta n(x)$, where *x* is the coordinate perpendicular to the semiconductor-dielectric-metal interface. It should be noted that silicon solar cells with photoconversion efficiency $\eta \ge 20\%$ have bulk lifetimes in excess of 1 ms. Therefore, the criterion $L_d >> d$ is well fulfilled in them. In this paper, we perform simulations and quantitatively describe the experimental results obtained in Ref. [1].

2. Quantum output and short-circuit current

The external quantum output $EQE(\lambda)$ enables to determine the short-circuit current density for incident radiation with the photon flux spectral density $I(\lambda)$ as

$$J_{SC} = q\int d\lambda\, EQE(\lambda)\, I(\lambda)\,, \qquad (1)$$

where *q* is the elementary charge. The value of $EQE(\lambda)$ is defined by such factors as the chemical composition and morphology of the surface, the presence of a coating with transparent conductive or transparent layers or a grid for collecting current, the coefficient of light absorption in the semiconductor, and others.

In the works [8, 9], a theoretical approach is proposed, which allows one to simulate the value J_{SC}, having dependences for $EQE(\lambda)$ and for the light reflection coefficient $R(\lambda)$ in the device structure. In [3], we proposed a simplified approach that allows one to obtain the value J_{SC} and its dependence on the base thickness *d* for textured SC, operating only with the $EQE(\lambda)$ dependence. Its essence is as follows. To theoretically describe the behavior of $EQE(\lambda)$ near the absorption edge, an expression of the following form is used

$$q(\lambda, Z_{eff}, d) = \left[1 + 1/Z_{eff}\,\alpha(\lambda)\,d\right]^{-1}, \qquad (2)$$

where $q(\lambda, Z_{eff}, d)$ is the limiting value of the quantum efficiency in the absence of losses due to reflection, shading and absorption of light outside the base area of SC, λ – wavelength of illumination, Z_{eff} – effective light amplification factor in the textured SC, $\alpha(\lambda)$ – light absorption coefficient in the SC base.

Amplification of light in the SC base is caused by multiple diffuse reflections at different angles from the front and back surfaces into SC.

For the case of perfectly diffuse Lambertian reflection, when the limiting value of the amplification factor Z_m is equal to $4n_r^2(\lambda)$ [10, 11], where $n_r(\lambda)$ is the refractive index of silicon, the relationship between Z_{eff} and Z_m has the form

$$Z_{eff} = Z_m/b\,, \qquad (3)$$

where *b*, a numerical coefficient, is higher than unity. The value *b* characterizes the degree of deviation of the value of light amplification coefficient from the ideal Lambertian one.

The following procedure is proposed to find the dependence $EQE(\lambda, d)$. It is believed that in the long-wave absorption region ($\lambda \ge 850$ nm) the value $EQE_l(\lambda, d)$ is described by the following formula

$$EQE_l(\lambda, d) = \frac{f}{1 + 1/Z_{eff}\,\alpha(\lambda)\,d}\,, \qquad (4)$$

where *f* is a parameter less than unity. This parameter takes into account photocurrent losses due to shading, light reflection, and light absorption outside α-Si:H–c-Si.

It is taken into account that in the range of $\lambda \le 850$ nm the experimental value $EQE_k(\lambda)$ does not depend on the thickness, but is defined only by the losses due to reflection, shading and absorption of light outside the base region of SC. At the point $\lambda = 850$ nm, the values *EQE* are merging, which allows us to determine the coefficient *f*. For example, let's perform the procedure described above for solar cells [1] with the thickness values 45.7, 96.6, 194, and 394 µm (see Fig. 6).

Fig. 1 shows the experimental dependences $EQE(\lambda)$ for these SC and the calculated dependences $EQE_l(\lambda, d)$ consistent with the experimental ones. In the particular case under consideration, agreement between experiment and theory for all SCs occurs at values of *f* that lie in the range from 0.943 to 0.95. The larger the thickness of SC, the higher the value *f*, which correlates with the dependences for total photocurrent losses depending on the thickness, shown in Fig. 7b of the work [1].

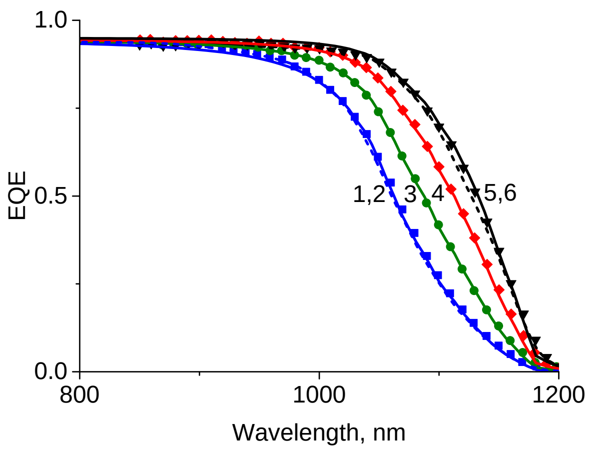

Fig. 1. Experimental and calculated dependences of $EQE(\lambda)$ for four SCs with the thicknesses of 45 (blue *1*), 96 (green *3*), 194 (red *4*), and 394 µm (black *5*) and the theoretical dependences of $EQE(\lambda)$ obtained by the authors [1] for SCs with the thicknesses of 45 (blue dotted line *2*) and 394 µm (black dotted line *6*).

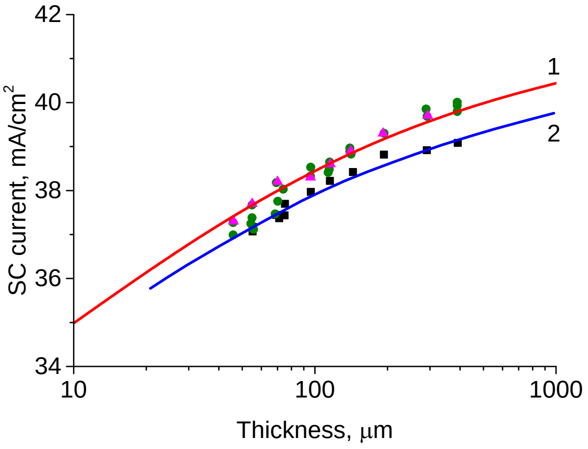

Fig. 2. Experimental and calculated dependences of the short-circuit current density on the thickness. The upper theoretical curve *1* was calculated by us, and the lower one *2* – by the authors [1].

Using the expression (3) gives the coefficient b equal to 2.2.

By separating the value $EQE(\lambda)$ into two components and substituting in (1), one can calculate the dependence $J_{SC}(d)$:

$$J_{SC}(d,b)=q\left[\int_{\lambda_0}^{850} I(\lambda)EQE(\lambda)d\lambda+\int_{850}^{1200} I(\lambda)EQE_l(\lambda,b)d\lambda\right]. \qquad (5)$$

Fig. 2 shows the experimental dependences of the photocurrent density on the SC thickness taken from Table 1 (see [1]), the experimental dependences $J_{SC}(d)$ shown in Fig. 4A, as well as theoretical dependences obtained using formulas (1)–(5). As it can be seen from the figure, the agreement between experiment and theory is good. It is important that agreement is obtained using only one key parameter, the coefficient b.

At the same time, the experimental dependences $J_{SC}(d)$ taken from Fig. 7A of [1] and the theoretical dependence $J_{SC}(d)$ obtained by the authors using the calculated data shown in Fig. 6 differ from that obtained by us. The reason for this difference, in our opinion, is that the use of the approach [2] gives approximate results, and the obtained error increases with an increase in the thickness of SC.

In particular, as it can be seen from the comparison of the theoretical dependences $EQE(\lambda)$ shown in Fig. 1, if for SC with the thickness 45 μm the theoretical dependences obtained by the ray tracing method coincide with those obtained in our approach, then for SC with a thickness of 394 μm they are noticeably different. At the same time, the difference between the short-circuit current densities obtained in our approach and in the ray tracing approach at 394 μm reaches approximately 20%.

3. Lifetimes in silicon

The total lifetime in silicon SC is formed by non-removable and removable recombination mechanisms [3]

$$\tau_{eff}^{-1}=\tau_{intr}^{-1}+\tau_{extr}^{-1}, \qquad (6)$$

where

$$\tau_{intr}=\left(\tau_{rad}^{-1}+\tau_{\text{Auger}}^{-1}\right)^{-1} \qquad (7)$$

is the lifetime for non-removable recombination mechanisms, which includes radiative recombination and interband Auger recombination, τ_{extr} – lifetime for removable recombination mechanisms, which includes the Shockley–Reed–Hall lifetime τ_{SRH}, the lifetime of non-radiative exciton recombination by the Auger mechanism with participation of a deep recombination level τ_{exc}^{n} [5], the lifetime due to surface recombination τ_{eff}^{s} and the lifetime due to recombination in the space charge region τ_{SCR}. In general

$$\tau_{extr}=\left(\tau_{\text{SRH}}^{-1}+\left(\tau_{eff}^{s}\right)^{-1}+\left(\tau_{exc}^{n}\right)^{-1}+\left(\tau_{SCR}\right)^{-1}\right)^{-1}. \qquad (8)$$

It should be noted that the latter two components are not taken into account in the currently existing theoretical approaches to calculating the key parameters of high-efficiency silicon solar cells.

Let us first focus on the justification of the need to take into account the mechanism of non-radiative exciton recombination according to the Auger mechanism with participation of deep recombination levels. In silicon, as it was shown for the first time in the works of Hangleiter [12, 13], in addition to the mechanisms of Shockley–Reed–Hall recombination and surface recombination, as well as mechanisms of radiative recombination and interband Auger recombination, there is also an Auger mechanism of non-radiative exciton recombination involving the deep center.

It was experimentally confirmed in the work by Fossum [14]. Together with the Shockley–Reed–Hall recombination mechanism, it was written in the form $\tau_{eff}=\tau_{\max}/(1+n_0/n_x)$, where $\tau_{\max}$ is the maximum value of the lifetime of minority charge carriers, n_0 is the doping level, and $n_x = 7.1\cdot10^{15}$ cm^{-3}. This mechanism was also taken into account in the PC1D program, but, unfortunately, the dependences of lifetime on the doping level proposed in [14] and used in the PC1D program were considered empirical.

In the work [5], this deficiency was corrected, and it was shown that the expression proposed, in particular, in the work [14], is not just empirical, but corresponds to the manifestation of the Auger mechanism of non-radiative exciton recombination involving the deep center according to the works [12, 13]. In the work [5], a number of experimental works were also analyzed, in which its existence is confirmed, being based on the analysis of which a refined coefficient n_x equal to $8.2\cdot10^{15}$ cm^{-3} was determined.

It should be noted that the monograph [15] devoted to presentation of materials on non-radiative recombination, also described the results of Hangleiter's work [12, 13] and the conditions for the manifestation of the mechanism of non-radiative exciton recombination involving the deep centers in silicon. In this work, the contribution of the indicated recombination mechanism together with other recombination mechanisms to the photoconversion efficiency of silicon SC was analyzed.

As for the mechanism related with the recombination in SCR, as it will be shown below, without taking it into account, a good theoretical agreement with the experiment cannot be obtained for a number of characteristics of silicon SCs, in particular, for the light *I–V* and the dependence of the output power when loading SC on voltage on it. In this work, this thesis will be confirmed for SC studied in the work [1].

The lifetime of radiative recombination is defined by the expression [3]

$$\tau_{rad}^{-1} = B\left(1 - P_{PR}\right)\left(n_0 + \Delta n\right), \tag{9}$$

where B is the parameter of radiative recombination in silicon, and P_{PR} is the probability of photon reabsorption, n_0 is the equilibrium concentration of electrons in the SC base, Δn is the excess concentration of electron-hole pairs. For B the relations are valid

$$B = \int_0^\infty dE\; B(E),$$

where

$$B(E) = \left(\frac{n_r(E)\,\alpha(E)\,E}{\pi\, c\, \eta^{3/2}\, n_i}\right)^2 e^{-E/k_B T}. \tag{10}$$

Here, $n_r(E)$ and $\alpha(E)$ are the refractive index and absorption coefficients as a function of photon energy $E = hc/\lambda$.

The value of the probability of reabsorption of photons is defined as

$$P_{PR} = B^{-1}\int_0^\infty dE\; A_{bb}(E)\, B(E). \tag{11}$$

In the approximation that $Z_{eff} = 4\,n_r(\lambda)^2/b$, the value $A_{bb}(E)$ is equal to

$$A_{bb}(E) = \frac{\alpha}{\alpha + \alpha_{FCA} + \left(4 n_r(\lambda)^2\, d/b\right)^{-1}}. \tag{12}$$

The second term in the denominator of the first fraction is the absorption coefficient on free charge carriers.

The expression (12) differs from that given in the work [17], there it introduces the coefficient b larger than unity. If the value α_{FCA} is neglected, as compared to α, then the expression (13) turns into (2).

For the lifetime of interband Auger recombination, we used the empirical expression given in [18].

The value of the Shockley–Reed–Hall lifetime depending on the doping level and the excitation level in the *n*-type semiconductor is described by the expression

$$\tau_{\mathrm{SRH}} \cong \frac{\tau_{p0}\left(n_0 + n_1 + \Delta n\right) + \tau_{n0}\left(p_1 + \Delta n\right)}{\left(n_0 + \Delta n\right)}, \tag{13}$$

where $\tau_{p0} = \left(V_p \sigma_p N_t\right)^{-1}$, $\tau_{n0} = \left(V_n \sigma_n N_t\right)^{-1}$, V_p and V_n are the average velocities of holes and electrons, σ_p and σ_n are the capture cross-sections of holes and electrons by the recombination levels, N_t – concentration of the recombination level, n_1 and p_1 – concentrations of electrons and holes in the case when the energy position of the recombination level coincides with the Fermi level. Depending on the excess concentration of electron-hole pairs Δn, the value τ_{SRH} changes between these two values – low-injection and high-injection ones.

The time of non-radiative exciton Auger recombination according to [8] is equal to

$$\tau_{exc}^{n} = \tau_{\mathrm{SRH}}\frac{n_x}{n_0 + \Delta n}, \tag{14}$$

where $n_x = 8.2\cdot 10^{15}$ cm^{-3}.

The lifetime due to surface recombination τ_{eff}^{s} is defined as

$$\tau_{eff}^{s} = \left(\frac{S_S}{d}\right)^{-1}, \tag{15}$$

where S_S is the total value of surface recombination rates on the front and back surfaces.

Next, we specify the dependence of the surface recombination rate on the level of excitation S and on the level of doping. We will assume that the value S_s is defined by the expression

$$S_s = S_{s0}\left(\frac{n_0}{n_p}\right)^m \left(1 + \frac{\Delta n}{n_0}\right)^r, \tag{16}$$

where S_{s0} is the total value of surface recombination rates on the front and back surfaces at a low level of excitation, n_p is the initial value of the doping level, $m \cong 1$ and the value r for most textured SCs is also equal to unity, however, as the experiment shows, there are individual cases when its value is smaller or larger than unity.

The lifetime due to recombination in SCR τ_{SCR} is defined as

$$\tau_{SCR} = \left(\frac{S_{SC}}{d}\right)^{-1}, \tag{17}$$

where S_{SC} is the rate of recombination in SCR.

In most of the materials used for the manufacturing textured silicon SC, the dependences $\tau_{eff}(\Delta n)$ in the region $\Delta n \le 10^{15}$ cm^{-3} saturate. At the same time, in the ready silicon textured SC, the decrease in the value $\tau_{eff}(\Delta n)$ with decreasing Δn is observed in the indicated region (see, for example, the work [19]). How are these two cases different? There is no *p-n* junction in the crystalline silicon samples used for measurements of $\tau_{eff}(\Delta n)$. On both surfaces of the sample, the band bends are symmetrical and, as a rule, they are depleted and low. In this case, recombination in SCR is practically absent.

At the same time, in the case of SC, there is a *p-n* junction on one of the SC surfaces. In this case, in the near-surface SCR of the *p-n* junction, recombination in SCR is significant. In the works [6, 7], we performed studies in which it was shown that the section in the dependence of the dark recombination current on the voltage applied to silicon SC is defined by recombination in SCR not only in the region of sufficiently small values V (0.4 V). It can be implemented up to the voltage values at the point of maximum power selection, when $V = V_m$ ($V_m = 0.55…0.65$ V).

This circumstance is explained by the fact that the value of the Shockley–Reed–Hall lifetime in SCR is always significantly less than the Shockley–Reed–Hall lifetime in the neutral bulk [6, 20]. In its turn, this is caused by the fact that the concentration of deep levels, which determine the lifetime τ_{SRH} in SCR, due to various reasons, turns out to be much higher than the concentration of deep levels in the neutral bulk.

A similar situation appears when silicon is passivated with the layers of SiN_x or Al_2O_3 (see, for example, [20, 21]), when a significant charge is built into the dielectric. In case of SiN_x, this charge is positive and in the case of Al_2O_3, it is negative. Then near the surface of *p*-type silicon in the first case and *n*-type silicon in the second case, conductivity inversion appears and recombination in SCR becomes significant.

In [20, 21] and in other works devoted to passivation of the silicon surface with dielectrics, this fact was confirmed primarily by the fact that in the dependence of the effective lifetime on excess concentration, there were observed a maximum and a decrease of τ_{eff} in the region Δn smaller than 10^{15} cm^{-3}. In the works mentioned above, the total value of the rate of surface recombination and recombination in SCR were taken into account to describe the dependences $\tau_{eff}(\Delta n)$. In our case, we do not combine and analyze them separately. At the same time, in these works, the influence of recombination in SCR on the key parameters of SC, for example, on the photoconversion efficiency, was not taken into account.

The value of the recombination rate in SCR S_{SC} was calculated using the expression

$$S_{SC}(\Delta n) = \int_0^w \frac{(n_0+\Delta n)dx}{\left[\left((n_0+\Delta n)e^{y(x)} + n_i(T)\exp\left(\frac{E_t}{kT}\right)\right) + b_r\left((p_0+\Delta n)e^{-y(x)} + n_i(T)\exp\left(-\frac{E_t}{kT}\right)\right)\right]\tau_R}. \quad (18)$$

Here, $C_n = V_{nT}\sigma_n$, $C_p = V_{pT}\sigma_p$ are the coefficients, σ_n and σ_p are the capture cross-sections of electrons and holes by the deep level, V_{nT} and V_{pT} are the average thermal velocities of electrons and holes, $b_r = C_p/C_n$, $\tau_R = \left(C_p N_t^*\right)^{-1}$ are the lifetime in SCR, N_t^* is the concentration of the deep level in SCR, $y(x)$ is the equilibrium volume concentration of holes, E_t – dimensionless electrostatic potential (band bending) in SCR, energy of the deep level in the silicon SCR, calculated from the middle of the band gap, $n_i(T)$ – concentration of own charge carriers, and w – thickness of SCR.

Passing from integration along the coordinate x to integration along the potential y, we get

$$S_{SC}(\Delta n) = \int_{y_w}^{y0} \frac{(n_0+\Delta n)dy}{\left[\left((n_0+\Delta n)e^{y} + n_i(T)\exp\left(\frac{E_t}{kT}\right)\right) + b_r\left((p_0+\Delta n)e^{-y} + n_i(T)\exp\left(-\frac{E_t}{kT}\right)\right)\right]\tau_R} F, \quad (19)$$

where

$$F = \frac{L_D}{\left[(1+\Delta n/n_0)\left(e^y - 1\right) + y_m + \left(\frac{p_0}{n_0} + \Delta n/n_0\right)\left(e^{-y} - 1\right)\right]^{1/2}}. \quad (20)$$

Here, $L_D = \left(\varepsilon_0\varepsilon_{Si} kT/2q^2 n_0\right)^{1/2}$ is the Debye length, q is the elementary charge, y_0 is the non-equilibrium dimensionless bending of the bands on the surface of the weakly doped region, which depends on the excitation level Δn and is found from the equation of integral neutrallity, y_w is the non-equilibrium dimensionless potential at the boundary of SCR near the quasi-neutral region.

To find the dependence of the non-equilibrium dimensionless potential y on the coordinate x, it is necessary to use the solution of the Poisson equation (the second integral) that has the following form

$$x = \int_{y_0}^{y} \frac{L_D}{\left[\left(1+\frac{\Delta n}{n_0}\right)\left(e^{y_1} - 1\right) - y_1 + \frac{\Delta n}{n_0}\left(e^{-y_1} - 1\right)\right]^{0.5}} dy_1 . \quad (21)$$

The value of the non-equilibrium dimensionless potential y_0 at $x = 0$ is found from the solution of the integral electroneutrality equation, which has the form

$$N = \pm\left(\frac{2kT\varepsilon_0\varepsilon_{\mathrm{Si}}}{q^2}\right)^{1/2}\begin{bmatrix}(n_0+\Delta n)\left(e^{y_0}-1\right)-\\ n_0 y_0+\Delta n\left(e^{-y_0}-1\right)\end{bmatrix}^{1/2}, \quad (22)$$

where qN is the surface density of charge of acceptors in the *p-n* junction or in the anisotypic heterojunction.

In the analytical approximation, the following expression is valid for the recombination rate in SCR

$$S_{SC}^{a}(\Delta n) \approx \frac{kL_{\mathrm{D}}}{\tau_R}\times$$
$$\times\frac{\exp(y_m)}{\left[(1+\Delta n/n_0)\left(e^{-y_m}-1\right)+y_m+\left(\frac{p_0}{n_0}+\Delta n/n_0\right)\left(e^{y_m}-1\right)\right]^{1/2}}, \quad (23)$$

where k is the numerical coefficient close to 2, and $y_m = (1/2)\ln\left((n_0+\Delta n)/b_r(p_0+\Delta n)\right)$.

The expression (23) can be used, if $y_m > 2$.

4. Modeling of open-circuit voltage and photo-conversion efficiency under AM1.5 conditions

We are dealing with SC, which is built on the basis of the p^+-i-α-Si:H/n-c-Si/i-n^+-α-Si:H structure. As it was shown in [22], the magnitude of the open-circuit voltage V_{OC} in silicon p^+-n-n^+ structures is determined using the expression:

$$V_{OC} \cong \frac{kT}{q}\ln\left(1+\frac{\Delta n_{OC}}{p_0}\right)+\frac{kT}{q}\ln\left(1+\frac{\Delta n_{OC}}{n_0}\right), \quad (24)$$

where Δn_{OC} is the concentration of excess charge carriers under open-circuit conditions, $p_0 = n_i^2(T,\Delta E_g)/n_0 = n_{i0}(T)^2\exp(\Delta E_g/kT)/n_0$ is the equilibrium concentration of holes in the *n*-type base, $\Delta E_g(n_0+\Delta n)$ is the narrowing of the gap width in silicon, calculated in [23], $n_{i0}(T)$ is the value of the concentration of own charge carriers in the absence of band narrowing [24].

Note that when the condition $L_d >> d$ is met, where L_d is the diffusion length of excess electron-hole pairs, and d is the thickness of the base, the criterion $\Delta n_{OC} > n_0$ is usually fulfilled. When the condition $L_d >> d$ is fulfilled, the value of Δn_{OC} can be found from the balance equation

$$J_{SC}/q = \left[\frac{d}{\tau_{eff}(\Delta n_{OC})}\right]\Delta n_{OC}, \quad (25)$$

where J_{SC} is the short-circuit current density, and the value $\tau_{eff}(\Delta n_{OC})$ is defined by expression (6), if we put Δn equal to Δn_{OC} in it.

The light *I–V* characteristic is determined using the following expressions

$$I_L(V) = I_{SC} - I_r(V) + \frac{V+IR_s}{R_{SH}}, \quad (26)$$

$$I_r(V) = qA_{SC}\left(\frac{d}{\tau_{eff}^{b}}+S_{00s}\left(1+\frac{\Delta n}{n_0}\right)+S_{SC}\right)\Delta n(V), \quad (27)$$

$$\tau_{eff}^{b}(n) = \left[\frac{1}{\tau_{\mathrm{SRH}}}+\frac{1}{\tau_{exc}^{n}(n)}+\frac{1}{\tau_{rad}(n)}+\frac{1}{\tau_{\mathrm{Auger}}(n)}\right]^{-1}, \quad (28)$$

$$\Delta n(V) = -\frac{n_0}{2}+\sqrt{\frac{n_0^2}{4}+n_i(T,\Delta E_g)^2\left(\exp\frac{q(V+IR_s)}{kT}-1\right)}, \quad (29)$$

where $I(V)$ is the total current, I_{SC} is the short-circuit current, $I_r(V)$ is the recombination (dark) current, A_{SC} is the SC area, V is the applied voltage, R_s and R_{SH} are the series and shunt resistance.

From the expression (29), we can also obtain the relation for the open-circuit voltage, if we put $I = 0$, and $\Delta n(V) \equiv \Delta n_{OC}$, accordingly, we have

$$V_{OC} = \frac{kT}{q}\ln\left(1+\frac{\Delta n_{OC}(n_0+\Delta n_{OC})}{n_i(T)^2\exp(\Delta E_g/kT)}\right). \quad (30)$$

By multiplying the current $I_L(V)$ by the applied voltage V, one can get the power $P(V)$, and from the condition of maximum dP/dV find the value of the voltage at the point of selection of the maximum power V_m. Substituting V_m into the equation (26), one obtains the value of current at the maximum power selection point I_m. This allows one to calculate the photo-conversion efficiency η and the filling factor FF in the usual way:

$$\eta = \frac{J_m V_m}{P_s}, \quad (31)$$

where P_s is the surface power density of illumination incident on SC in AM1.5 conditions.

$$FF = \frac{J_m V_m}{J_{SC}V_{OC}}. \quad (32)$$

5. Simulation results and their comparison with the experimental data

5.1. Dependence of the open-circuit voltage on the thickness of SC

Fig. 3 shows the experimental dependence of the open-circuit voltage on the SC thickness obtained in [1] and shown in Fig. 4b. The same figure shows the experimental dependence [1] obtained from Table.

The value $V_{OC}(d)$ was calculated using the expression (26) by substituting the following recombination parameters into it: τ_{SRH} = 200 ms [1], $\tau_R = 2\cdot10^{-5}$ s, b_r = 0.1, y_w = –0.03. During the calculations, it was assumed that the energy of the deep levels responsible for recombination in SCR E_t is close to the middle of the band gap. Then the second terms in the first and second brackets of the denominator (19) can be neglected. Fig. 4 shows the theoretical dependences $S_{SC}(\Delta n)$ obtained using the formulas (19), (23) using the above parameters and the value of the coefficient k equal to 2.

When calculating the dependence, two cases were considered. In the first of them, the value b_r = 0.1 was used in the calculation, and in the second, the value b_r = 1, when the hole capture coefficient is equal to the electron capture coefficient $C_p = C_n$. In the second case, the value $\tau_R = 10^{-5}$ s was also used for calculation. As can be seen from the figure, the values of S_{SC} calculated using Exps (19) and (23) in the current region of excess concentrations $5\cdot10^{13} < \Delta n < 5\cdot10^{13}$ cm^{-3} are quite close.

In further calculations, we used the dependences obtained from the formula (19) when using the values $\tau_R = 1\cdot10^{-5}$ and b_r = 0.1. Plotted in the inset to Fig. 4 dependences of $S_{SC}(\Delta n)\cdot\tau_R$, at different values of the doping level, when N_d is assumed to be equal to 10^{14}, 10^{15}, 10^{16}, 10^{17} cm^{-3}, if using the following parameters: b_r = 1, y_w = –0.1. The dependences obtained in this case are identical to the dependences shown in Fig. 2.25 of the work [20].

To theoretically determine the value of the surface recombination rate $S_S(\Delta n)$, it is necessary to determine the low-signal surface recombination rate S_{s0} and the proportionality coefficient r. This problem is solved for each SC, the light current characteristics of which are shown in Fig. 2 in the work [1], separately. The value of S_{s0} is selected in such a way that the calculated value V_{OC} for SC of a certain thickness coincides with the value given in the table of work [1]. At the same time, it was assumed that the coefficient r is equal to unity.

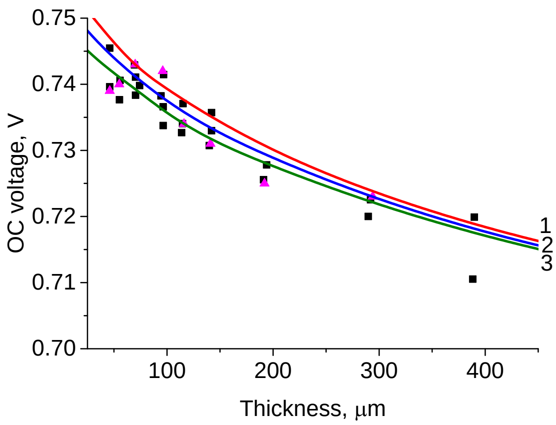

Fig. 3. Experimental and theoretical dependences of open-circuit voltage on thickness. The theoretical dependences are given using SC parameters with the thicknesses of 70 (*1*), 294 (*2*), and 116 µm (*3*).

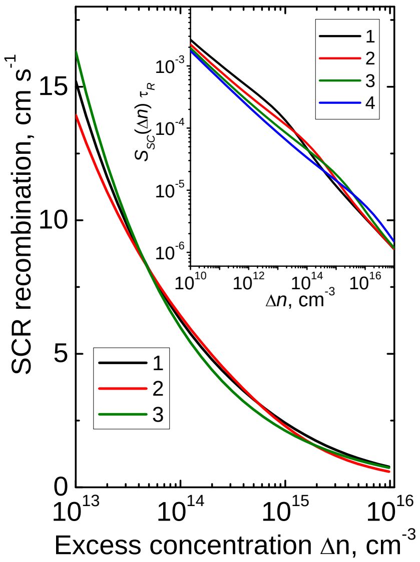

Fig. 4. Theoretical dependences plotted using the expressions (19) – red *1*, blue *2* curves and (23) – green *3* curve. The value of the ratio of hole-to-electron capture coefficients is b_r = 0.1 (*1* – red curve), b_r = 1 (*2* – blue curve). Insert to Fig. 4. Dependences of $S_{SC}(\Delta n)\cdot\tau_R$ at different values of the doping level, when N_d is assumed equal to 10^{14} (*1* – black), 10^{15} (*2* – red), 10^{16} (*3* – green), and 10^{17} cm^{-3} (*4* – blue).

The obtained values of S_{s0} are shown in Table. After that, the theoretical dependences of $V_{OC}(d)$ can be calculated. Shown in Fig. 3 are both experimental values and theoretical dependences of $V_{OC}(d)$. Note that the same $S_{SC}(\Delta n)$ was used in the calculations for each SC. The following arguments serve as a basis for that.

The value of S_{SC} depends on the level of doping and on the characteristics of SCR. In the case when the inversion of conductivity, which occurs for SC, is realized in SCR, the S_{SC} ceases to depend on the characteristics of SCR. Therefore, the dependence of $S_{SC}(\Delta n)$ for all three SCs with the same level of doping should be the same. As can be seen from Fig. 3, the agreement between experimental and theoretical dependences of $V_{OC}(d)$ is quite good. Also, the figure shows that the larger the value of S_{s0}, the smaller the value of V_{OC}.

Fig. 5 shows the theoretical dependences for the effective lifetime τ_{eff} on the excess concentration for three SCs, the light *I–V* characteristics of which are shown in Fig. 2 (Ref. [1]). As can be seen from the figure, in the region of $\Delta n < 10^{15}$ cm^{-3}, the values of τ_{eff} decrease with decreasing Δn, which is caused by the effect of recombination in SCR.

In some cases, the dependence of $\tau_{eff}(\Delta n)$ with its maximum can be realized due to the fact that the bulk lifetime is not constant, but increases with growing Δn. In *n*-type silicon, this situation can be realized, when the gold level takes part [8]. It is possible to distinguish these two cases, when the maximum $\tau_{eff}(\Delta n)$ is related to the influence of recombination in SCR, or to the dependence of $\tau_{SRH}(\Delta n)$, by measuring the dependences of $\tau_{eff}(\Delta n)$ at

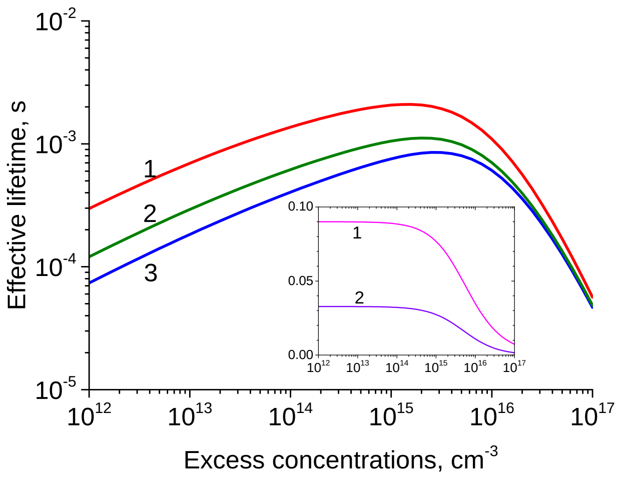

Fig. 5. Theoretical dependences of the effective lifetime on the excess concentration for SC with thicknesses of 294 (red *1*), 116 (green *2*), and 70 μm (blue *3*). The inset shows the time of radiative recombination (pink curve *1*) and the time of non-radiative recombination (purple curve *2*) as a function of Δn.

small excess concentrations. When the recombination occurs in SCR, the values of $\tau_{eff}(\Delta n)$ decrease as Δn decreases all the time, while in the second case, with sufficiently small values of Δn, the value of τ_{eff} reaches saturation.

In the inset to Fig. 5, the theoretical dependences for the time of radiative recombination and the time of excitonic non-radiative recombination depending on the excess concentration Δn for SC with the thickness 116 μm are presented. As can be seen from the figure, these times are of the same order, in particular, at $\Delta n = 10^{12}$ cm^{-3} their ratio is equal to 2.68, that is, the contribution of exciton non-radiative recombination to the total lifetime is larger.

According to the analysis carried out in [5], as the Shockley–Reed–Hall lifetime increases, the contribution of excitonic non-radiative recombination to the photo-conversion efficiency decreases, and at τ_{SRH} = 20 ms it is sufficiently small, but it increases with an increase in the level of doping, and at $n_0 = 2.4\cdot10^{15}$ cm^{-3}, its fraction is 0.29 of τ_{SRH}, *i.e.* 5.8 ms. This value is usually greater than the measurement errors of τ_{SRH}.

5.2. Photoconversion efficiency

Now let's move to the theoretical calculation of the photoconversion efficiency for the indicated three SCs. To perform the calculation, it is necessary to know the shunt and series resistance values for each SC. The value of the shunt resistance for each SC sample is found graphically from the slope of the light *I*–*V* characteristic in the region of low applied voltages by using the expression

$$R_{SH} = -\left(\frac{dJ_L}{dV}\right)^{-1}_{V=0}. \qquad (33)$$

Unfortunately, the accuracy of the $J_L(V)$ dependences measured in [1] in the vicinity of $V = 0$ is insufficient to directly use the expression (33) to find R_{SH}. Therefore, we found these values for three experimental SCs by using two points in the $J_L(V)$ dependences within the region where the indicated dependences are close to the linear ones. The second point in the $J_L(V)$ dependence was chosen from the condition that $\Delta J_L(V_2) >> J_{SC}$.

The question of the unequivocal solution in this case remains open. However, taking into account the fact that when the obtained values of R_{SH} change into their increase, the light *I*–*V* characteristic changes very weakly, it is possible to solve the main task of the work, *i.e.*, to demonstrate that without taking into account recombination in SCR, the experimental and theoretical *I*–*V* characteristics cannot be agreed with each other.

After that, one unknown parameter remains – series resistance. And then we proceed in the same way as before, that is, we find it by fitting the theoretical and experimental values of η. Table shows the values of S_{s0}, R_{SH} and R_s for three SCs, the light *I*–*V* characteristic of which are shown in Fig. 2 from the paper [1].

Fig. 6 shows the experimental dependences for light *I*–*V* characteristics taken from Fig. 2 of the paper [1], and theoretical dependences were constructed using the above parameters in the region $V > 0.6$ V. As can be seen from the figure, the agreement between experiment and theory is good. When plotting the figure, the lifetime in SCR τ_R for SC with thicknesses 294 and 116 μm was assumed to be equal to 10 μs, and for SC with the thickness from 70 μm to 8 μs.

In the same figure, the theoretical dependences of the light *I*–*V* characteristics are presented, in the con-struction of which recombination in SCR was neglected, but the surface recombination rate and the series resistance

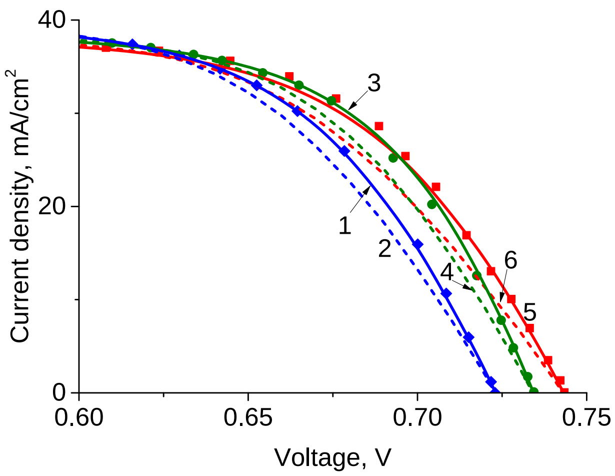

Fig. 6. Experimental (points) and theoretical (lines) dependences for light *I*–*V* characteristics of SC with the thickness 70 (red squares), 116 (green circles), and 294 μm (blue rhombs). Dashed curves (*2*, *4*, *6*) correspond to the case when recombination in SCR is not taken into account, and solid curves (*1*, *3*, *5*) to the case when it is taken into account.

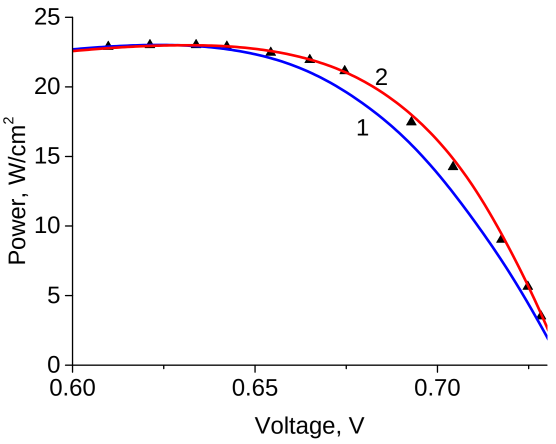

Fig. 7. Experimental (points) and theoretical (lines) dependences for the loading characteristic of SC with the thickness 116 μm. Blue line (*1*) corresponds to the case when recombination in SCR is not taken into account, and red line (*2*) – to the case when it is taken into account.

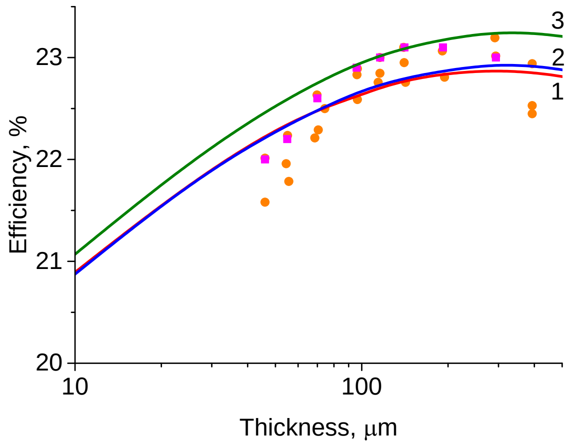

Fig. 8. Experimental (points) and calculated (lines) photoconversion efficiency *vs* the base thickness. Theoretical dependences are plotted for the agreed SC parameters with the thickness 70 (red *1*), 116 (green *3*) and 294 μm (blue *2*).

were corrected so that the experimental and theoretical values of η coincided. As can be seen from the figure, in this case $V \le V_m$, the theoretical dependences obtained with and without taking into account recombination in SCR coincide, but they diverge at $V > V_m$. We note that the values of V_m for the studied SC are close to 0.63 V. The dependences obtained when recombination in SCR is not taken into account, at the same time, are lower than the experimental ones. Fig. 7 shows experimental and calculated loading characteristics for SC with the thickness 294 μm. As can be seen from the figure, in the case when recombination in SCR is taken into account, the experimental and calculated load dependences coincide, and in the case when it is not taken into account, after the maximum power selection point, the calculated dependences are lower than the experimental ones. The same picture is true for the other two SCs.

Load dependences were calculated using the formula

$$P(V) = J_L(V)V \, . \tag{34}$$

The table also shows the values of the photoconversion efficiency for the three SCs studied in [1], and the value of changes in the photoconversion efficiency for these SCs in the cases where recombination in SCR ($\Delta\eta_1$) (or surface recombination ($\Delta\eta_2$)) is not taken into account. As can be seen from the table, the changes in efficiency when recombination in SCR (or surface recombination) is not taken into account are of the same order, but the effect of recombination in SCR on the photoconversion efficiency is larger.

In the latter two rows of the table, respectively, the changes in the photoconversion efficiency for the investigated SCs are presented, without taking into account excitonic non-radiative recombination $\Delta\eta_{exc}$ and the effect of band narrowing $\Delta\eta_{zn}$. As can be seen from the table, the changes in photoconversion efficiency, when excitonic non-radiative recombination is not taken into account, are larger than the changes related with not taking into account the effect of band narrowing. Thus, it can be concluded that if the band narrowing effect is taken into account, it is necessary to take into account non-radiative exciton recombination.

As the calculations showed, the photoconversion efficiency investigated in the work [1] SC within the interval $10^{14}\ldots5\cdot10^{15}$ cm^{-3} depends very weakly on the level of doping. So, for example, the difference between the maximum and minimum value of photoconversion efficiency for SC with the thickness 294 μm is 0.4%, while for SC with thicknesses of 70 and 116 μm it is about 0.2%.

Table. Some parameters of SC studied in the work [1] and changes in the photoconversion efficiency, when recombination in SCR or surface recombination is not taken into account.

No	d, μm	R_{SH}, Ω·cm^2	R_s, Ω·cm^2	S_0, cm/s	η, %	$\Delta\eta_1$, %	$\Delta\eta_2$, %	$\Delta\eta_{exc}$, %	$\Delta\eta_{zn}$, %
1	70	9520	0.685	0.945	22.6	0.83	0.57	0.047	0.146
2	116	4967	0.55	1.41	23.0	0.66	0.63	0.054	0.141
3	294	4120	0.67	1.54	23.0	0.55	0.37	0.092	0.147

On the one hand, at low levels of doping, this is due to a weak dependence of the recombination rate in SCR on the level of doping. While at medium and higher levels of doping, this is due to the fact that the increase in the open-circuit voltage with an increase in the level of doping is compensated by the increase in the rate of surface recombination.

Fig. 8 shows the experimental and calculated thickness dependences of the photoconversion efficiency for two SCs studied in [1]. As can be seen from the figure, the experimental and theoretical dependences $\eta(d)$ correlate well with each other. The parameter that defines the differences between the calculated dependences $\eta(d)$ is series resistance. The smaller it is, the larger the values of η.

Thus, the above results indicate that in the high-efficient silicon-based SCs studied in [1], along with other recombination mechanisms, recombination in SCR plays a significant role. Its contribution is commensurate with that of other recombination mechanisms, in particular, with the contribution of surface recombination, and without taking it into account it is impossible to obtain good agreement between the experimental light *I–V* characteristics and the loading characteristics with the theory.

The same conclusion takes place for other high-efficiency textured SC based on silicon, the characteristics of which were simulated by us in previous works, and in them, taking into account recombination in SCR, agreement between experiment and theory was achieved for the dark *I–V* characteristics, as well as for the dependences $J_{SC}(V_{OC})$.

6. Conclusions

So, as the results of this work showed, the used theory allows quantitative description of the experimental results obtained in the work [1]. It is applicable both to the thickness dependences of short-circuit current, open-circuit voltage, and photoconversion efficiency, as well as to light *I–V* characteristics and dependences of the output power in the SC load on the voltage on it, studied in the work [1].

It has been shown that the latter two characteristics can be quantitatively agreed with the theory, only if recombination in SCR is taken into account. In this work, we have obtained correct expressions for the recombination rate in SCR, which are valid not only for small values of the concentration of electron-hole pairs Δn, when the inequality $\Delta n < n_0$ is fulfilled, but also in the range of values Δn, where the inverse relationship is fulfilled.

This paper shows that the contribution of non-radiative Auger exciton recombination with participation of a deep impurity level in silicon (see the work [1]) is of the same order as the contribution of radiative recombination. Also, it has been shown that taking the non-radiative exciton recombination into account reduces the photoconversion efficiency more than taking the band narrowing effect into account. The similar results were obtained in the works [4–6], which once again proves the need to take into account the mentioned recombination mechanism. The results obtained in the work can be used to optimize the characteristics of textured silicon SC, in particular, in terms of thickness.

References

1. Sai H., Oku T., Sato Y. *et al.* Potential of very thin and high efficiency silicon heterojunction solar cells. *Prog. Photovolt. Res. Appl*. 2019. **27**. P. 1061–1070. https://doi.org/10.1002/pip.3181.
2. Wafer ray tracer version 1.6.7. https://www2.pvlighthouse.com.au/calculators. Publ. 2015.
3. Sachenko A.V., Kostylyov V.P., Sokolovsky I.O., Evstigneev M. Effect of temperature on limit photoconversion efficiency in silicon solar cells. *IEEE J. Photovolt.* 2020. **10**, No 1. P. 63–69. https://doi.org/10.1109/JPHOTOV.2019.2949418.
4. Sachenko A.V., Kostylyov V.P., Bobyl A.V. *et al.* The effect of base thickness on photoconversion efficiency in textured silicon-based solar cells. *Tech. Phys. Lett.* 2018. **44**, No 10. P. 873–876. https://doi.org/10.1134/S1063785018100139.
5. Sachenko A.V., Kostylyov V.P., Vlasyuk V.M. *et al.* The influence of the exciton nonradiative recombination in silicon on the photoconversion efficiency. *Proc. 32 European Photovoltaic Solar Energy Conf. and Exhib*., Germany, Munich, 20–24 June, 2016. P. 141–147. https://doi.org/10.4229/EUPVSEC20162016-1BV.5.14.
6. Sachenko A.V., Kostylyov V.P., Vlasiuk V.M. *et al.* Features in the formation of recombination current in the space charge region of silicon solar cells. *Ukr. J. Phys.* 2016. **61**, No 10. P. 917–922. https://doi.org/10.15407/ujpe61.10.0917.
7. Sachenko A.V., Kostylyov V.P., Sokolovsky I.O. Specific features of current flow in α-Si:H/Si heterojunction solar cells. *Tech. Phys. Lett.* 2017. **43**. P. 152–155. https://doi.org/10.1134/S1063785017020109.
8. McIntosh K.R. and Baker-Finch S.C. A parameterization of light trapping in wafer-based solar cells. *IEEE J. Photovolt.* 2015. **5**, No 6. P. 1563–1570. https://doi.org/10.1109/JPHOTOV.2015.2465175.
9. Fell A., McIntosh K.R. and Fong K.C. Simplified device simulation of silicon solar cells using a lumped parameter optical model. *IEEE J. Photovolt.* 2016. **6**, No. 3. P. 611–616. https://doi.org/10.1109/JPHOTOV.2016.2528407.
10. Tiedje T., Yablonovitch E., Cody G.D. and Brooks B.J. Limiting efficiency of silicon solar cells. *IEEE Trans. Electron. Devices*. 1984. **ED31**, No 5. P. 711–716. https://doi.org/10.1109/T-ED.1984.21594.
11. Green M.A. Lambertian light trapping in textured solar cells and light-emitting diodes: Analytical solutions. *Prog. Photovolt.: Res. Appl.* 2002. **10**, No 4. P. 235–241. https://doi.org/10.1002/pip.404.

12. Hangleiter A. Nonradiative recombination *via* deep impurity levels in silicon: Experiment. *Phys. Rev. B*. 1987. **35**, No 17. P. 9149–9161. https://doi.org/10.1103/physrevb.35.9149.
13. Hangleiter A. Nonradiative recombination via deep impurity levels in semiconductors: The excitonic Auger mechanism. *Phys. Rev. B*. 1988. **37**, No 5. P. 2594–2604.
14. Fossum J.G. *Solid State Electron*. Computer-aided numerical analysis of silicon solar cells. 1976. **19**, No 4. P. 269–277. https://doi.org/10.1016/0038-1101(76)90022-8.
15. Abakumov V.N., Perel V.I., Yassievich I.N. *Nonradiative Recombination in Semiconductors*. Elsevier Science, 1991.
16. Richter A., Glunz S.W., Werner F. *et al*. Improved quantitative description of Auger recombination in crystalline silicon. *Phys. Rev. B*. 2012. **86**. P. 165202. https://doi.org/10.1103/PhysRevB.86.165202.
17. Richter A., Hermle M., Glunz S.W. Reassessment of the limiting efficiency for crystalline silicon solar cells. *IEEE J. Photovolt.* 2013. **3**. P. 1185–1191. https://doi.org/10.1109/JPHOTOV.2013.2270351.
18. Richter A., Benick J., Feldmann F. *et al*. *n*-type Si solar cells with passivating electron contact: Identifying sources for efficiency limitations by wafer thickness and resistivity variation. *Sol. Energy Mater. Sol. Cells*. 2017. **173**. P. 96–105. https://doi.org/10.1016/j.solmat.2017.05.042.
19. Yoshikawa K., Yoshida W., Irie T. *et al*. Exceeding conversion efficiency of 26% by heterojunction interdigitated back contact solar cell with thinfilm Si technology. *Sol. Energy Mater. Sol. Cells.* 2017. **173**. P. 37–42. https://doi.org/10.1016/j.solmat.2017.06.024.
20. Dauwe S. Low-temperature surface passivation of crystalline silicon and its application to the rear side of solar cells. *PhD thesis*, Universität Hannover, 2004.
21. Veith-Wolf B.A. Crystalline silicon surface passivation using aluminum oxide: Fundamental understanding and application to solar cell. *PhD thesis*, Universität Hannover, 2018.
22. Gorban A.P., Sachenko A.V., Kostylyov V.P. and Prima N.A. Effect of excitons on photoconversion efficiency in the p^+-n-n^+ and n^+-p-p^+ structures based on single-crystalline silicon. *SPQEO.* 2000. **3**, No 3. P. 322–329. https://doi.org/10.15407/spqeo3.03.322.
23. Schenk A. Finite-temperature full random-phase approximation mode of band gap narrowing for silicon device simulation. *J. Appl. Phys*. 1998. **84**. P. 3684–3695. https://doi.org/10.1063/1.368545.
24. Sproul A.B. and Green M.A. Intrinsic carrier concentration and minority-carrier mobility of silicon from 77 to 300 K. *J. Appl. Phys*. 1993. **73**. P. 1214. https://doi.org/10.1063/1.353288.

Authors and CV

Sachenko A.V. Professor, Doctor of Physics and Mathematics Sciences, Chief Researcher at the Laboratory of Physical and Technical Fundamentals of Semiconductor Photovoltaics at the V. Lashkaryov Institute of Semiconductor Physics. He is the author of more than 300 scientific publications. His main research interests include analysis, characterization, and modeling of silicon solar cells.
E-mail: sach@isp.kiev.ua;
https://orcid.org/0000-0003-0170-7625

Kostylyov V.P. Professor, Doctor of Physics and Mathematics Sciences, Head at the Laboratory of Physical and Technical Fundamentals of Semiconductor Photovoltaics at the V. Lashkaryov Institute of Semiconductor Physics. He is the author of more than 250 scientific publications. The area of his scientific interests includes photovoltaics and betavoltaics, research, analysis and modeling of solar cells, characterization and testing the solar cells, as well as characterization of the optical and recombination properties of photovoltaics materials.
E-mail: vkost@isp.kiev.ua;
https://orcid.org/0000-0002-1800-9471

Vlasiuk V.M. PhD, Senior Researcher at the Laboratory of Physical and Technical Fundamentals of Semiconductor Photovoltaics at the V. Lashkaryov Institute of Semiconductor Physics. He is the author of more than 60 scientific publications. The area of his scientific interests includes research, analysis of silicon solar cells.
https://orcid.org/0000-0001-6352-0423

Sokolovskyi I.O. PhD, Senior Researcher at the Laboratory of Physical and Technical Fundamentals of Semiconductor Photovoltaics at the V. Lashkaryov Institute of Semiconductor Physics. He is the author of more than 70 scientific publications. His main research interests include modeling of silicon solar cells.
E-mail: falcon128@gmail.com,
https://orcid.org/0000-0002-7072-6670

Evstigneev M.A. Assistant Professor of the faculty of Physics and Physical Oceanography at the Memorial University of Newfoundland. His research areas are non-equilibrium statistical physics, biophysics, surface science.
E-mail: mevstigneev@mun.ca,
https://orcid.org/0000-0002-7056-2573

Slusar T.V. Senior Researcher at Electronics and Telecommunications Research, Daejeon, South Korea. The area of her scientific interests includes thin films and waveguides fabrication, solar cells, strongly-correlated materials, non-linear and quantum optics. E-mail: tslusar@etri.re.kr,
https://orcid.org/0000-0001-8837-6165

Chernenko V.V. Senior Researcher at the Laboratory of Physical and Technical Fundamentals of Semiconductor Photovoltaics, V. Lashkaryov Institute of Semiconductor Physics. He is the author of more than 100 scientific publications. His main research interests include research, analysis of silicon solar cells.
E-mail: vvch@isp.kiev.ua,
https://orcid.org/0000-0002-7630-6925

Authors' contributions

Sachenko A.V.: formulation of the problem, analysis, investigation, data curation (partially), writing – original draft, writing – review & editing, visualization.
Kostylyov V.P.: conceptualization, methodology, validation, analysis, data curation, writing – original draft, writing – review & editing.
Vlasiuk V.M.: conceptualization, investigation, writing – review & editing, project administration.
Sokolovskyi I.O.: investigation, resources, software.
Evstigneev M.: analysis, validation, writing – review & editing.
Slusar T.V.: investigation, validation, resources.
Chernenko V.V.: investigation, discussed the results, resources.
All authors discussed the results and commented on the manuscript.

Моделювання характеристик високоефективних текстурованих сонячних елементів на основі кристалічного кремнію. Вплив рекомбінації в області просторового заряду

А.В. Саченко, В.П. Костильов, В.М. Власюк, І.О. Соколовський, М.О. Євстігнєєв, Т.В. Слюсар, В.В. Черненко

Анотація. У роботі виконано теоретичне моделювання оптичних і фотоелектричних характеристик високоефективних текстурованих кремнієвих сонячних елементів (СЕ), таких, зокрема, як струм короткого замикання, напруга розімкненого кола та ефективність фотоперетворення. При моделюванні додатково враховано такі рекомбінаційні механізми як безвипромінювальна екситонна рекомбінація за механізмом Оже за участю глибокого рекомбінаційного рівня та рекомбінація в області просторового заряду (ОПЗ). У простому наближенні змодельовано зовнішній квантовий вихід фотоструму для вказаних СЕ у довгохвильовій області поглинання. Запропоновано теорію для розрахунку товщинних залежностей струму короткого замикання, напруги розімкненого кола та ефективності фотоперетворення в них. Розраховані залежності ретельно порівняно з експериментальними результатами, отриманими для СЕ з архітектурою p^+-i-α-Si:H/n-c-Si/i-n^+-α-Si:H та ефективністю фотоперетворення близько 23%. У результаті порівняння отримано добре узгодження між теоретичними та розрахунковими залежностями. Установлено, що без урахування рекомбінації в ОПЗ не може бути отримано кількісне узгодження між експериментальними та теоретичними світловими ВАХ і залежностями вихідної потужності у навантаженні СЕ від напруги на ньому. Запропонований підхід і отримані результати можуть бути використані для оптимізації характеристик текстурованих СЕ на основі монокристалічного кремнію.

Ключові слова: кремнієвий сонячний елемент, теоретичне моделювання, зовнішній квантовий вихід фотоструму, струм короткого замикання, напруга розімкненого кола та ефективність фотоперетворення.